Have CO_2 emissions from land use change systematically been underestimated?

A Arneth (1), S Sitch (2), J Pongratz (3), B Stocker (4,5), P Ciais (6), B Poulter (7), A Bayer (1), A Bondeau (8), L Calle (7), L. Chini (9), T Gasser (6), M Fader (8,10), P Friedlingstein (11), E Kato (12), W Li (6), M Lindeskog (13), J E M S Nabel (3), TAM Pugh (1, 14), E Robertson (15), N Viovy (6), C Yue (6), S Zaehle (16)

(1) Karlsruhe Institute of Technology, Dept. Atmospheric Environmental Research, Kreuzeckbahnstr. 19, 82467 Garmisch-Partenkirchen, Germany

(2) College of Life and Environmental Sciences, University of Exeter, Exeter, EX4 4RJ, UK

(3) Max Planck Institute for Meteorology, Bundesstr. 53, 20146 Hamburg, Germany

(4) Department of Life Sciences and Grantham Institute for Climate Change, Imperial College London, Silwood Park, Ascot, SL5 7PY, UK

(5) Institute for Atmospheric and Climate Science, ETH Zürich, Universitätstrasse 16, 8092 Zürich, Switzerland

(6) IPSL – LSCE, CEA CNRS UVSQ, Centre d'Etudes Orme des Merisiers, 91191 Gif sur Yvette France

(7) Institute on Ecosystems and Department of Ecology, Montana State University, Bozeman, MT 59717

(8) Institut Méditerranéen de Biodiversité et d'Ecologie marine et continentale, Aix-Marseille Université, CNRS, IRD, Avignon Université, Technopôle Arbois-Méditerranée, Bâtiment Villemin, BP 80, 13545 Aix-en-Provence CEDEX 04, France

(9) Department of Geographical Sciences, University of Maryland, College Park, MD 20742, USA

(10) International Centre for Water Resources and Global Change, hosted by the German Federal Institute of Hydrology. Am Mainzer Tor 1, 56068 Koblenz, Germany

(11) College of Engineering, Mathematics and Physical Sciences, University of Exeter, Exeter, EX4 4QE, UK

(12) The Institute of Applied Energy, Minato, Tokyo 105-0003, Japan

(13) Dept of Physical Geography and Ecosystem Science, Sölvegatan 12, Lund University, 22362 Lund, Sweden

(14) School of Geography, Earth & Environmental Sciences and Birmingham Institute of Forest Research, University of Birmingham, Birmingham, B15 2TT, United Kingdom

(15) Met Office Hadley Centre, FitzRoy Road, Exeter, EX1 3PB, UK

(16) Max Planck Institute for Biogeochemistry, 07701 Jena, Germany

The terrestrial biosphere absorbs about 20% of fossil fuel CO_2 emissions. The overall magnitude of this sink is constrained by the difference between emissions, the rate of increase in atmospheric CO_2 concentrations and the ocean sink. However, the land sink is actually composed of two largely counteracting fluxes that are poorly quantified: fluxes from land-use change and CO_2 uptake by terrestrial ecosystems. Dynamic global vegetation model simulations suggest that CO_2 emissions from land-use change have been substantially underestimated because processes such as tree harvesting and land-clearing from shifting cultivation have not been considered. Since the overall terrestrial sink is constrained, a larger net flux as a result of land-use change implies that terrestrial uptake of CO_2 is also larger, and that terrestrial ecosystems might have greater potential to sequester carbon in the future. Consequently, reforestation projects and efforts to avoid further deforestation could represent important mitigation pathways, with co-benefits for biodiversity. It is unclear whether a larger land carbon sink can be reconciled with our current understanding of terrestrial carbon cycling. In light of our possible underestimation of the historical residual terrestrial carbon sink and associated uncertainties, we argue that projections of future terrestrial carbon uptake and losses are more uncertain than ever.

The net atmosphere-to-land carbon flux (F_{L}) is typically inferred as the difference between relatively well-constrained terms of the global carbon cycle: fossil fuel and cement emissions, oceanic carbon uptake and atmospheric growth rate of CO_2 (see Textbox) [1]. In contrast, very large uncertainties exist in how much anthropogenic land-use and land-cover change (F_{LULCC}) contributes to F_{L}, which propagates into large uncertainties in the estimation of the 'residual' F_{RL} (see Box). The lack of confidence in separating F_{L} into its component fluxes diminishes the predictive capacity for terrestrial carbon cycle projections into the future. It restricts our ability to estimate the capacity of land ecosystems to continue to mitigate climate change, and to assess land management options for land-based mitigation policies.

As land-use change emissions and the residual sink are spatially closely enmeshed, global-scale observational constraints do not exist for estimating F_{LULCC} or F_{RL} separately. Dynamic Global Vegetation Models (DGVMs) have over recent years been used to infer the magnitude and spatial distribution of F_{LULCC} as well as of F_{RL}, while F_{LULCC} has traditionally been also derived from data-driven approaches such as the bookkeeping method [1-3] (see Box). Although large, for many sources of uncertainties in F_{LULCC} there is no good reason to believe that these would introduce a systematic under- or overestimation[4-6]. However, until recently, most processes related to land management and the subgrid-scale dynamics of land-use change have been ignored in large-scale assessments of the terrestrial carbon balance, and we argue here that including these missing processes might systematically increase the magnitude of F_{LULCC}. In turn, an upward revision of F_{LULCC} implies through the global budget the existence of a substantially higher F_{RL} and raises the question whether a larger F_{RL} is plausible given our understanding of the response of ecosystems to changing environmental conditions.

Accounting for gross land-cover transitions, such as shifting cultivation (*SC*)

Opposing changes in different land-use types can take place simultaneously within a region (see methods, and Supplementary Figure), e.g. an area is converted from natural to managed land, whereas an equal area within the same region might be abandoned or reforested, equating to a net zero land-cover change. The magnitude of these bi-directional changes depends on the size of the area investigated. Over thousands of km^2, the typical resolution of DGVMs, ignoring sub-grid changes can have a substantial effect on the simulated carbon cycle, since accounting for the gross changes (e.g., the parallel conversion to, and abandonment of, agricultural land in the same grid-cell) includes (rapid) carbon losses from deforestation, (slow) loss from post-deforestation soil legacy effects, and (slow) uptake in areas of regrowth. In sum this leads to younger mean stand-age, smaller biomass pools and thus higher F_{LULCC} compared to net area-change simulations.

Gross area transitions are fundamental to LULCC dynamics in areas of shifting cultivation in the tropics[7], but also occur elsewhere[8]. Gross forest loss far exceeding net area loss can be demonstrated from remote-sensing products globally[9], although these products in themselves cannot distinguish effects of logging from natural disturbance events such as fire or storms. Secondary forests in the tropics can return to biomass carbon stocks comparable to old-growth forest within 5-6 decades[10], but the same is not the case for soil carbon. Also, fallow lengths in shifting cultivation systems tends to be shorter, and show a decreasing trend in many regions[11]. These dynamics result in the degraded vegetation and reduced soil carbon stocks commonly observed in disturbed forest land [12].

Wood harvest (*WH*)

Until recently, global DGVM studies that accounted for LULCC concentrated on the representation of conversion of natural lands to croplands and pastures, while areas under forest cover were represented as natural forest, and hence by each model's dynamics of establishment, growth and mortality. Two thirds to three quarters of global forests have been affected by human use, mainly harvest, as a source of firewood, roundwood and secondary products, or for recreational purposes [13]. Between 1700-2000 an estimated 86 PgC has been removed globally from forests due to wood harvest [14], and presently around 10% of the net primary production appropriated by humans is by forestry, ca. 1.3 Pg C a^{-1} . Wood harvest leads to reduced carbon density on average in managed forests [15] and can ultimately result in degradation in the absence of sustainable management strategies. Furthermore, the harvest of wood can reduce litter input, which lowers soil pools[13]. The effect of bringing a natural forest under any harvesting regime will be net CO_2 emissions to the atmosphere, its time-dependency depending on harvest intensity and frequency, regrowth, and by the fate and residence time of the wood products.

Pastures grazing and crop harvest (*GH*), and cropland management (*CP*)

Management is not only fundamental for the carbon balance of forests, but also for pasture and cropland. As with forests, accounting for management processes on arable lands has only recently been included in DGVMs (see methods). Regular grazing and harvesting (*GH*), and more realistic crop processes (*CRP*) such as flexible sowing and harvesting, or tillage, will enhance F_{LULCC} [16]. Over decadal timescales, conversion of forest to cropland has been observed to reduce soil carbon pools by around 40% [17], resulting from reduced vegetation litter soil inputs and enhanced soil respiration in response to tillage, although the effect and magnitude of the latter is being debated [18] . Conversion to pasture often has either little effect, or may even increase soil carbon [17].

Impacts of land management processes on the carbon cycle

The few DGVM studies published that include more realistic processes for the management of land[,16,19-21] consistently suggest a systematically larger F_{LULCC} over the historical period compared to estimates that ignored these , with important implications for our understanding of the terrestrial carbon cycle and its role for historical (and future) climate change. In order to assess if results from these initial experiments hold despite differences among models, we compile here results from a wider set of DGVMs (and one DGVM "emulator", see methods and Supplementary Table 1), adopting the approach described in [2]. F_{LULCC} was calculated as the difference between a simulation in which CO_2 and climate were varied over the historical period, at constant (pre-industrial) land use, and one in which land use was varied as well.

When accounting for shifting cultivation and wood harvest, F_{LULCC} was systematically enhanced (Fig. 1). *SC*,, without the possibility of shade-trees remaining in cultivated areas, sincreased cumulative F_{LULCC} over the period 1901-2014 on average by 35 ± 18 PgC (Fig. 1; Supplementary Table 2). While three DGVMs had demonstrated this effect previously[19-21], an upward shift of F_{LULCC} was also found in the other models that performed additional *SC* simulations for this study. Including wood harvest caused F_{LULCC} to increase over the same time period by a similar magnitude to *SC*, 30 ± 21 PgC. Trends in *WH*-related F_{LULCC} over time differed between models (Fig. 1) likely due to different rates of post-harvest regrowth, and assumptions about residence time in different pools[22]. Including the harvest of crops and the grazing of pastures also resulted in larger F_{LULCC}, since carbon harvested or grazed is consumed and released as CO_2 rapidly instead of decaying slowly as litter and soil organic matter. Beyond harvest, accounting for more realistic cropland management such as tillage processes (*CRP*) also showed, with one exception (in which tillage effects were not modelled, see methods) an enhancement of F_{LULCC} emissions.

When ignoring the additional land-use processes investigated here, average F_{LULCC} is 119 ± 50 PgC (Supplementary Table 2). Adding effects of *SC*, *WH*, *GH* and *CRP* enhance land-use change emissions by, on average, 20-30% each (Fig. 2; Supplementary Table), with individually large uncertainties. The total effects on F_{LULCC} are difficult to judge as models do not yet account for all land-use dynamics. For instance, *SC* and *WH* effects are expected to enhance F_{LULCC} additively as there is little overlap in the input dataset used by DGVMs regarding the areas that are assumed to be under shifting cultivation, and areas where wood harvest occurs [7]. But in the case of *GH* and *CRP,* carbon cycle interactions with *SC* and *WH* cannot be excluded because subsequent transitions could occur in a grid location, between primary vegetation and cropland, pastures or secondary forests. The overall enhancement of F_{LULCC} therefore will need to be explored with model frameworks that include all dynamic land-use change processes. DGVMs currently contributing to the annual update of the global carbon budget account for some of the processes examined here, but as yet not at all comprehensively, and we thus expect DGVM-based F_{LULCC} to increase substantially compared to results reported in[1]. As a consequence the discrepancy to book-keeping estimates of F_{LULCC} will become larger, although results in [23] call for a broader range of book-keeping approaches as well.

Implications for the residual land sink over the historical period

In order to match F_{L} in the global carbon budget (Box) for the historical period a substantially larger F_{LULCC} would need to be balanced by a corresponding increase in F_{RL}, which could be either due to underestimated historical increase in GPP and vegetation biomass, overestimated heterotrophic carbon loss, or both. The question arises if such a discrepancy is credible in light of today's understanding. [24] [12526]

The response of photosynthesis to increasing CO_2 could underlie more than half of today's land carbon sink [27]. Several recent lines of observation-based evidence suggest that GPP may have undergone much stronger enhancement over the last century than currently calculated by DGVMs. These studies include isotopic analysis of herbarium plant samples, of stable oxygen isotope ratios in atmospheric CO_2, and accounting for the effect of leaf mesophyll resistance to CO_2 [28-30]. Ciais et al. [31] inferred a pre-industrial GPP of 80 PgC a^{-1} based on measurements of oxygen isotopes in ice-core air, indicative for a 33% difference to the often-used present-day GPP benchmark of ca. 120 PgC a^{-1} [32] and independently consistent with the 35% increase suggested by [28]. In contrast, the participating DGVMs in this study show an average increase of GPP by only 15% between the first and last ten years of the simulation (not shown).

Whether or not enhancements in GPP translate into increased carbon storage depends on other factors such as nutrient and water supply, seen for instance in the mixed trends in stem growth found in forest inventories [33,34]. Much work remains to better understand the response of ecosystem carbon storage to increasing atmospheric CO_2 concentration [35]. Ultimately, enhanced growth will only result in increasing carbon pools if turnover time does not increase at the same rate [22]. Besides GPP and heterotrophic ecosystem respiration (ER), lateral carbon flows play an important role in the ecosystem carbon sink. Recent syntheses that combined a range of observations, inventories of carbon stock changes, trade flows and transport in waterways, estimated dissolved organic carbon losses to account for a flux of > 1.0 PgC a^{-1}, with an unknown historical trend [36,37]. The fate of this carbon is highly uncertain, but its inclusion would enhance the calculated residual sink via an additional source term (eqn. 1, textbox).

Taken together, a number of candidates for underestimated F_{RL} in today's models are plausible, and a combination of the above listed processes likely. It remains to be seen whether a larger F_{LULCC} can be supported by observation-based estimates. Using emerging constraints, Li et al. und enhanced LULCC emissions when historical DGVM estimates were forced by present-day forest biomass from a range of inventories and remote sensing, even though their analysis is based on regressions obtained from models that also exclude part of the processes investigated here. Thus several lines of evidence suggest that a common low-bias in the historic F_{LULCC} could affect all DGVMs, and the challenge of resolving the many open issues will stay with us for some years to come.

How do unknowns in historical LULCC reconstructions fit into the picture?

Patterns and historical trends of deforestation, cropland and pasture management or wood harvest are uncertain. Land use reconstructions differ substantially in terms of the time, location and rate of LULCC (see [38] and reference therein). The DGVM and climate science community has mostly relied on the LUH1 data-set by Hurtt et al. [7], chiefly because it provides the needed seamless time-series from the historical period into future projections at the spatial resolution required by DGVMs. Clearly such a globally applicable, gridded data-set must necessarily include simplifications. For instance, the assumed uniform 15-year turnover in tropical shifting cultivation systems[7] cannot account for the known variation between a few years and one to two decades, or trends towards shorter fallow periods in some regions (see [11] and references therein), while there is also an increasing proportion of permanent agriculture. Likewise, not only the amount of wood harvest but also the type of forestry (coppice, clear-cut, selective logging, fuel-wood) will vary greatly in time and space, which is difficult to hindcast [39,40].

In upcoming revisions to LUH1 (LUH-2, http://luh.umd.edu/data.shtml), forest-cover gross transitions are now constrained by the remote sensing information[9], and have overall been re-estimated (Fig. 3). Whether or not this will result in reduced *SC* carbon loss estimates in recent decades remains to be seen. At the same time, these historical estimates consider large gross transitions of land-cover change only for tropical regions even though there is good reason to believe that bi-directional changes occur elsewhere[41]. For Europe alone, a recent assessment that is relatively impartial to spatial resolution estimated twice the area having undergone land-use transitions since 1900 when accounting for gross *vs*. net area changes[8]. This leads to substantial increase in the calculated historical European F_{LULCC}, both in a bookkeeping-model and DGVM-based study[42]. Historical land carbon cycle estimates therefore are not only highly uncertain due to missing LULCC processes, but equally so due to the LULCC reconstructions *per se*. However, for a given reconstruction, accounting for additional processes discussed here will always introduce a unidirectional enhancement in F_{LULCC} compared to ignoring these processes.

Implications for the future land carbon mitigation potential

Our calculated increases in F_{LULCC}, in absence of a clear understanding of the processes underlying F_{RL}, notably strengthen the existing arguments to avoid further deforestation (and all ecosystem degradation) – an important aspect of climate change mitigation, with considerable co-benefits to biodiversity and a broad range of ecosystem service supply. One could also conjecture whether or not a larger historical carbon loss through LULCC would imply a larger potential to sequester carbon through reforestation, than thought so far. However, assessments of mitigation potentials must consider the often relatively slow carbon gain in re-growing forests (compared to the rapid, large loss during deforestation), in particular the sluggish replenishment of long-term soil carbon storage [43,44]. What is more, trees grow now, and will in future, under very different environmental conditions compared to the past. A warmer climate increases mineralisation rates and hence enhances nutrient supply to plant growth, supporting the CO_2 fertilisation effect, but also stimulates heterotrophic decay of existing soil carbon and/or flow of dissolved carbon, with as yet no agreement about the net effects [3,45]. Re-growing forests might also in future be more prone to fire risk, and other episodic events such as wind-throw or insect outbreaks[46,47], crucial ecosystem features not yet represented well in models [48]. This question of “permanence” has been an important point of discussion at conferences under the UNFCCC, and also hampers of payment-for-ecosystem-services schemes that target conservation measures, since it is unclear how an increasing risk of losing carbon-uptake potential can be accounted for [49,50].

Given that we may be greatly underestimating the present-day F_{RL}, and therefore missing or underestimating the importance of key driving mechanisms, projections of future terrestrial carbon uptake and losses appear more fraught with uncertainty than ever. In the light of the findings summarised here, this poses not only a major challenge when judging mitigation efforts, but also for the next generation of DGVMs and Earth System models to assess the future global carbon budget. Future work therefore needs to concentrate on representing the interactions between physiological responses to environmental change in ecosystems with improved representations of human land management.

References

1 Le Quere, C. *et al.* Global Carbon Budget 2015. *Earth Sys. Sci. Data* 7, 349-396 (2015).

2 Sitch, S. *et al.* Recent trends and drivers of regional sources and sinks of carbon dioxide. *Biogeosciences* 12, 653-679 (2015).

3 Ciais, P. *et al.* in *Climate Change 2013: The Physical Science Basis. Contribution of Working Group I to the Fifth Assessment Report of the Intergovernmental Panel on Climate Change.* (eds T.F. Stocker *et al.*) (Cambridge University Press, 2013).

4 Pongratz, J., Reick, C., Houghton, R. A. & House, J. I. Terminology as a key uncertainty in net land use flux estimates. *Earth Syst. Dyn.* 5, 177-195 (2013).

5 Gasser, T. & Ciais, P. A theoretical framework for the net land-to-atmosphere CO_2 flux and its implications in the definitions of "emissions from land-use change". *Earth Syst. Dyn.* 4, 171-186 (2013).

6 Houghton, R. A. *et al.* Carbon emissions from land use and land-cover change. *Biogeosciences* 9, 5125-5142 (2012).

7 Hurtt, G. C. *et al.* Harmonization of land-use scenarios for the period 1500-2100: 600 years of global gridded annual land-use transitions, wood harvest, and resulting secondary lands. *Clim. Change* 109, 117-161 (2011).

8 Fuchs, R., Herold, M., Verburg, P. H., Clevers, J. G. P. W. & Eberle, J. Gross changes in reconstructions of historic land cover/use for Europe between 1900 and 2010. *Glob. Change Biol.* 21, 299-313 (2015).

9 Hansen, M. C., Stehman, S. V. & Potapov, P. V. Quantification of global gross forest cover loss. *Proc. Nat. Acad. Sci.* 107, 8650-8655 (2010).

10 Poorter, L. *et al.* Biomass resilience of Neotropical secondary forests. *Nature* 530, 211-214 (2016).

11 van Vliet, N. *et al.* Trends, drivers and impacts of changes in swidden cultivation in tropical forest-agriculture frontiers: A global assessment. *Glob. Env. Change* 22, 418-429 (2012).

12 Grace, J., Mitchard, E. & Gloor, E. Perturbations in the carbon budget of the tropics. *Glob. Change Biol.* 20, 3238-3255 (2014).

13 Erb, K.-H. *et al.* Land management: data availability and process understanding for global change studies. *Glob. Change Biol.*, gcb.13443 (2016).

14 Hurtt, G. C. *et al.* The underpinnings of land-use history: three centuries of global gridded land-use transitions, wood-harvest activity, and resulting secondary lands. *Glob. Change Biol.*, 12, 1208-1229 (2006).

15 Noormets, A. *et al.* Effects of forest management on productivity and carbon sequestration: A review and hypothesis. *For. Ecol. Manag.* 355, 124-140 (2015).

16 Pugh, T. A. M. *et al.* Carbon emission from land-use change is substantially enhanced by agricultural management. *Env. Res. Lett.*, 124008 (2015).

17 Guo, L. B. & Gifford, R. M. Soil carbon stocks and land use change: a meta analysis. *Glob. Change Biol.* 8, 345-360 (2002).

18 Powlson, D. S. *et al.* Limited potential of no-till agriculture for climate change mitigation. *Nat. Clim. Change* 4, 678-683 (2014).

19 Shevliakova, E. *et al.* Carbon cycling under 300 years of land use change: Importance of the secondary vegetation sink. *Glob. Biogeochem. Cycles* 23, GB2022 (2009).

20 Stocker, B. D., Feissli, F., Strassmann, K. M., Spahni, R. & Joos, F. Past and future carbon fluxes from land use change, shifting cultivation and wood harvest. *Tellus B* 66, 23188 (2014).

21 Wilkenskjeld, S., Kloster, S., Pongratz, J., Raddatz, T. & Reick, C. H. Comparing the influence of net and gross anthropogenic land-use and land-cover changes on the carbon cycle in the MPI-ESM. *Biogeosciences* 11, 4817-4828 (2014).

22 Friend, A. D. *et al.* Carbon residence time dominates uncertainty in terrestrial vegetation responses to future climate and atmospheric CO2. *Proc. Nat. Acad. Sci.* 111, 3280-3285 (2014).

23 Hansis, E., Davis, S. J. & Pongratz, J. Relevance of methodological choices for accounting of land use change carbon fluxes. *Glob. Biogeochem. Cycles* 29, 1230-1246 (2015).

24 Pan, Y. *et al.* A Large and Persistent Carbon Sink in the World's Forests. *Science* 333, 988-993 (2011).

25 Ahlström, A. *et al.* The dominant role of semi-arid ecosystems in the trend and variability of the land CO2 sink. *Science* 348, 895-899 (2015).

26 Erb, K.-H. *et al.* Bias in attributing of forest carbon sinks. *Nat. Clim. Change* 3, 854-856 (2013).

27 Schimel, D., Stephens, B. B. & Fisher, J. B. Effect of increasing CO2 on the terrestrial carbon cycle. *Proc. Nat. Acad. Sci.* 112, 436-441 (2015).

28 Ehlers, I. *et al.* Detecting long-term metabolic shifts using isotopomers: CO2-driven suppression of photorespiration in C-3 plants over the 20th century. *Proc. Nat. Acad. Sci.* 112, 15585-15590 (2015).

29 Sun, Y. *et al.* Impact of mesophyll diffusion on estimated global land CO2 fertilization. *Proceedings of the National Academy of Sciences*, doi:10.1073/pnas.1418075111 (2014).

30 Welp, L. R. *et al.* Interannual variability in the oxygen isotopes of atmospheric CO2 driven by El Nino. *Nature* 477, 579-582 (2011).

31 Ciais, P. *et al.* Large inert carbon pool in the terrestrial biosphere during the Last Glacial Maximum. *Nat. Geosc.* 5, 74-79 (2012).

32 Beer, C. *et al.* Terrestrial Gross Carbon Dioxide Uptake: Global Distribution and Covariation with Climate. *Science* 329, 834-838 (2010).

33 McMahon, S. M., Geoffrey G Parker, and Dawn R Miller. 2010. . Evidence for a recent increase in forest growth. *Proc. Nat. Acad. Sci* 107, 3611–3615 (2010).

34 van der Sleen, P. *et al.* No growth stimulation of tropical trees by 150 Years of CO_2 fertilization but water-use efficiency increased. *Nat. Geosc.* 8, 24–28 (2015).

35 Pugh, T. A. M., Muller, C., Arneth, A., Haverd, V. & Smith, B. Key knowledge and data gaps in modelling the influence of CO2 concentration on the terrestrial carbon sink. *J. Plant Phys.* 203, 3-15 (2016).

36 Raymond, P. A. *et al.* Global carbon dioxide emissions from inland waters. *Nature* 503, 355-359 (2013).

37 Regnier, P. *et al.* Anthropogenic perturbation of the carbon fluxes from land to ocean. *Nat. Geosc.* 6, 597-607, doi:10.1038/ngeo1830 (2013).

38 Prestele, R. *et al.* Hotspots of uncertainty in land use and land cover change projections: a global scale model comparison. *Glob. Change Biol.*, gcb.13337 (2016).

39 Bais, A. L. S., Lauk, C., Kastner, T. & Erb, K. Global patterns and trends of wood harvest and use between 1990 and 2010. *Ecol. Econ.* 119, 326-337 (2015).

40 McGrath, M. J. *et al.* Reconstructing European forest management from 1600 to 2010. *Biogeosciences* 12, 4291-4316 (2015).

41 Richter, D. D. & Houghton, R. A. Gross CO2 fluxes from land-use change: implications for reducing global emissions and increasing sinks. *Carb. Manag.* 2, 41-47 (2011).

42 Bayer, A. D., Lindeskog, M., Pugh, T. A. M., Fuchs, R. & Arneth, A. Uncertainties in the land use flux resulting from land use change reconstructions and gross land transitions. *Earth Syst. Dyn. Discuss.* (2016).

43 Korner, C. Slow in, rapid out - Carbon flux studies and Kyoto targets. *Science* 300, 1242-1243 (2003).

44 Krause, A., Pugh, T. A. M., Bayer, A. D., Lindeskog, M. & Arneth, A. Impacts of land-use history on the recovery of ecosystems after agricultural abandonment. *Earth Syst. Dyn.* 7, 745-766 (2016).

45 Zaehle, S., Jones, C. D., Houlton, B., Lamarque, J.-F. & Robertson, E. Nitrogen Availability Reduces CMIP5 Projections of Twenty-First-Century Land Carbon Uptake. *J. Clim.* 28, 2494-2511 (2015).

46 Seidl, R., Schelhaas, M. J., Rammer, W. & Verkerk, P. J. Increasing forest disturbances in Europe and their impact on carbon storage. *Nat. Clim. Change* 4, 806-810 (2014).

47 Hantson, S. *et al.* The status and challenge of global fire modelling. *Biogeosciences* 13, 3359-3375 (2016).

48 Running, S. W. Ecosystem disturbance, carbon, and climate. *Science* 321, 652-653 (2008).

49 Galik, C. S., Murray, B. C., Mitchell, S. & Cottle, P. Alternative approaches for addressing non-permanence in carbon projects: an application to afforestation and reforestation under the Clean Development Mechanism. *Mitigation and Adaptation Strategies for Global Change* 21, 101-118 (2016).

50 Friess, D. A., Phelps, J., Garmendia, E. & Gomez-Baggethun, E. Payments for Ecosystem Services (PES) in the face of external biophysical stressors. *Glob. Env. Change* 30, 31-42 (2015).

Acknowledgements

AA, ADB and TAMP acknowledge support from EU FP7 grants LUC4C (grant no. 603542) and OPERAS (grant no.308393), and the Helmholtz Association in its ATMO programme and its impulse and networking fund. MF, WL, CY and SS were also funded by LUC4C. JP and JEMSN were supported by the German Research Foundation's Emmy Noether Program (PO

1751/1-1). EK was supported by the ERTDF (S-10) from the Ministry of the Environment, Japan. ER was funded by LUC4C and by the Joint UK DECC/Defra Met Office Hadley Centre Climate Programme (GA01101). SZ has received funding from the European Research Council (ERC) under the European Union‘s Horizon 2020 research and innovation programme (grant agreement no. 647204; QUINCY). BDS is supported by the Swiss National Science Foundation and FP7 funding through project EMBRACE (282672). PC received support from the ERC SyG project IMBALANCE-P ‘Effects of phosphorus limitations on Life, Earth system and Society’ Grant agreement no.: 610028.’

Author contributions

AA, SS, JP, BS conceived the study. BP, LC, AB, MF, EK, JEMN, ADB, ML, TAMP, ER, TG, NV, CY, SZ made changes to model code and provided simulation results. AA and SS analysed results. BS, PC, WL provided Fig. 3. AA wrote the first draft, all authors commented on the draft and discussion of results.

Textbox: Calculations of global terrestrial carbon uptake and removal

The net atmosphere-to-land carbon flux (F_{L}) is generally inferred as the difference between other terms of the global carbon cycle perturbation,

$$F_L = F_{FFC} - F_O - \frac{dA_{CO2}}{dt} \qquad (1)$$

where F_{FFC} are fossil fuel and cement emissions, F_{O} is the atmosphere-ocean carbon exchange (currently an uptake) and $\frac{dA_{CO2}}{dt}$ is the atmospheric growth rate of CO_2 (1). F_{FFC} and $\frac{dA_{CO2}}{dt}$ are well known, and the estimate of the decadal global ocean carbon sink is bounded by a range of observations[1] such that the net land carbon flux is relatively well constrained. By contrast, there is much less confidence in separating F_{L} into a carbon flux from anthropogenic land use and land cover change (F_{LULCC}), and a 'residual' carbon flux to the land ($F_{\mathrm{RL};}$ (2)) which is typically calculated as the difference from the other carbon-cycle components:

$$F_L = F_{RL} - F_{LULCC} \qquad (2)$$

F_{LULCC} and F_{LR} are both made up of source and sink fluxes. Uncertainties in F_{LULCC} and F_{RL} are around 35% - 40% over the period 1870-2014 (when expressed as % of the cumulative mean absolute values), compared to 13% for the cumulative ocean sink and 5% for fossil fuel burning and cement emissions[1].

F_{LULCC} has been modelled by the bookkeeping method (combining data-driven representative carbon stocks trajectories and/or –for the satellite period– remote-sensing information on carbon density for different biomes, with estimates of land-cover change), or by dynamic global vegetation models (DGVMs; calculating carbon density of ecosystems with process-based algorithms; see methods). DGVMs can also be used to calculate explicitly the magnitude and spatial distribution of F_{RL} [1,2] instead of deducing its global value as a difference between F_{L} and F_{LULCC} as done in global budget analyses. The bookkeeping approach has the advantage that carbon densities and carbon response functions that describe the temporal evolution and fate of carbon after a LULCC disturbance can be based directly on observational evidence [6,23], but has to assume that local observations can be extrapolated to regions/countries or biomes, thus partly ignoring spatial edaphic and climatic gradients of carbon stocks. The DGVM-based simulations have the advantage to account for environmental effects on carbon stocks through time, and account for spatial heterogeneity, but are poorly constrained by data. DGVMs and bookkeeping models have similarly large degree of uncertainties [1].

Figure captions

Figure 1: Difference in LULCC emission flux (Δ_{FLULCC}) due to individual processes. Coloured lines represent different models, grey symbols and hairlines are average ± one standard deviation.
a: wood harvest; b: shifting cultivation; c: harvest (using the grass functional type); d: full crop representation

Figure 2: Response ratio of cumulative $F_{\mathrm{LULCC},1}$ and $F_{\mathrm{LULCC},0}$. See also Supplementary Table 1 and methods for individual processes and models.

Figure 3: Comparison of net (a) and gross (b) forest / natural land change (in Million km^2) between different LULCC data sets. Changes in LUH1 data [7] represents the change of natural land because there is no separate forest type in LUH1 while change in the other data sets indicates the forest change.

Methods (and references for methods)

1) General simulation set-up

Carbon fluxes from land-use change are derived as the difference between a simulation with historically varying observed climate, atmospheric CO_2 concentration and land-cover change (S3) and one in which land-cover change was held constant (S2) [1,2]. Land-cover changes were taken from HYDE[3] or LUH1[4]. In S2, land-cover distribution was fixed. Gridded historical estimates of gross-transitions (shifting cultivation in the tropics; *SC*) and wood harvesting (*WH*) were taken from [4].

Spin up used repeated climate from the first decades of the 20th century, and constant CO_2 concentration and land-cover distribution (for details, see section 2). Upon achieving steady-state, land-cover distribution and CO_2 concentration were allowed to evolve transiently, whilst transient climate evolution began at 1901. Atmospheric CO_2 concentration was taken from ice core data until ca. mid-20th century, when atmospheric measurements became available[2]. A "baseline" carbon flux related to land-use change ($F_{\mathrm{LULCC},0}$; see Supplementary Table 1) is defined as excluding gross transitions and wood harvest, and using the grass plant functional type to represent crop areas. Data in this Perspective article were from previously published work, supplemented by from additional, new simulations. In cases where more than one of the processes that are under investigation here were assessed by one model several *S3* experiments were provided. While spin-up and model configurations differed between models, for S2 and S3 simulations of any one individual model the set-up was the same, which allows to identify the effect of adding the individual processes. Section (2) provides a brief summary of relevant aspects of models and simulation protocol, in particular where they differ from their previously published versions.

2) Individual models

2.1 JULES

Here, to implement crop harvest, four additional PFTs were added: C3 crops, C4 crops, C3 pasture and C4 pasture, with identical parameter sets as the C3 and C4 grass PFTs. Lotka-Volterra equations [5] are used three times to calculate the vegetation distribution in natural areas, crop and pasture areas, with the calculations in each area being independent of the others. Crop harvest is represented by diverting 30% of crop litter to the fast product pool instead of to the soil; the fast product pool has a rapid decay timescale of 1 year. Pasture is not harvested.

The model is forced by crop and pasture area from the Hyde 3.2 dataset [2] and by CRU-NCEP climate[1,2], both at 1.875x1.25 degrees, using an hourly time-step, and updating vegetation distribution every ten days. 1080 years of spin-up were run by fixing crop and pasture areas at 1860 levels and by repeating 1901-1920 climate and CO_2 concentrations.

2.2 JSBACH

The JSBACH version used here is similar to the version in [2]. S3 experiments include gross land-use transitions and wood harvest [6]. $F_{LULCCc,0}$ in Supplementary Table 2 were calculated by subtracting the individual contributions of these processes. Net transitions are derived from the gross transition implementation, but by minimizing land conversions [6]. Wood harvest [4] is taken not only from forest PFTs but also shrubs and natural grasslands are harvested. Upon harvest, 20% of the carbon is immediately released to the atmosphere; the rest is transferred into the litter and subject to soil dynamics. JSBACH simulations were conducted at 1.9°x1.9° forced with remapped 1° LUH1 data from 1860-2014 and daily climate calculated from the 6-hourly 0.5° CRU-NCEP product [2] for the years 1901-2014. The initial state in 1860 is based on a spin-up with 1860 CO_2 concentrations (286.42 ppm), cycling (detrended) 1901-1921 climate and constant 1860 LUH1 wood harvest amounts. From 1860 annual CO_2 forcing was used, and after 1901climate was taken from CRU-NCEP. In the no-harvest simulation the 1860 wood harvest amounts were applied throughout the whole simulated period.

2.3 LPJ-GUESS

SC: For implementing shifting cultivation, recommendations followed those by [4], with rotation periods of 15 years. Simulations used the coupled carbon-nitrogen version of the model [7-8] Spin-up used constant 1701 land-cover and CO_2 concentration, and 1901-1930 recycled climate. Upon steady-state land-cover and CO_2 were allowed to change from 1701, and climate from 1901 onwards[9]. When land is cleared, 76% of woody biomass and 71% of leaf biomass is removed and oxidised within one year, with a further 21 % of woody biomass assigned to a product pool with 25 year turnover time [9]. Upon abandonment a secondary forest stand is created and recolonization of natural vegetation takes place from a state of bare soil. With forest rotation, young stands (above a minimum age of 15 years) are preferentially converted.

GH/MC: Simulations are taken from [8], using the carbon-only version of the model. 68% of deforested woody biomass and 75% of leaf biomass is oxidised within one year, with a further 30% of woody biomass going to the product pool. In the *GH* case, 50% of the above-ground biomass are annually removed from the ecosystem. In MC, 90% of the harvestable organs and an additional 75% of above-ground crop residues are removed each year. Simulations ran from 1850 to 2012, with 1850 land-cover and CO_2 concentrations, and recycled climate (1901-1930) being used for spin-up.

All LPJ-GUESS simulations used CRU TS 3.23 climate [10].

2.4 LPJ

Compared to previous versions, the model now uses the World Harmonization Soils Database version 1.2 for soil texture and Cosby equations [11] to estimate soil water holding capacity. Further developments allow for gross land-use transitions and wood harvest to be prescribed. Changes include (1) the primary grid-cell fraction only decreases in size; (2) secondary grid-cell fractions can decrease or increase in size by combining with other secondary forest fractions, recently abandoned land, or fractions with recent wood harvest; (3) deforestation results in an immediate flux to the atmosphere equal to 100% of heartwood biomass and 50% of sapwood biomass; root biomass enters belowground litter pools, while 100% leaf and 50% of sapwood biomass becomes part of aboveground litter.

Wood harvest demand [4] on primary or secondary lands was met by the biomass in tree sapwood and heartwood only. Only whole trees were harvested (i.e., tree-density was reduced); wood from deforestation was not included to meet wood harvest demand. 100% of leaf biomass and 40% of the sapwood and heartwood enters the aboveground litter, and 100% of root biomass enters the belowground litter pools; 60% of sapwood and heartwood are assumed to go into a product pool. Of these, 55% go to the 1-year product pool (emitted in the same year), 35% go to the 10-year product pool (emitted at rate 10% per year) and 10% go to the 100-year product pool (emitted at rate 1% per year). These delayed pool-emission fluxes are part of the LULCC fluxes. After harvest, the harvested fraction is mixed with existing secondary forest fraction, or a secondary fraction is created if none exists, while fully conserving biomass. For simulations with shifting cultivation, grid-cell fractions that underwent land-use change were not mixed with existing managed lands or secondary fractions until all land-use transitions had occurred. Simulations were performed using monthly CRU [10] (TS3.23) climate at 0.5° degrees, and finished in year 2013. Spin-up was done using recycled 1901-20 climate, and using 1860 land-cover and CO_2. Upon steady-state, land cover and CO_2 varied after 1860 and climate varied after 1900.

2.5 LPJmL

The LPJmL version used was as described in [12-14]. In the baseline scenario all crops were simulated as a mixture of C3 and C4 managed grasslands, 50% of the aboveground biomass is transferred to the harvest compartment and assumed to be respired in the same year. Climate data was 1901-2014 CRU TS v. 3.23 monthly datasets and land-use patterns from the HYDE 3.2 dataset. Simulations were performed at 0.5° spatial resolution. Model spin-up used recycled climate data from 1901-1920, and with land use patterns and CO_2 concentrations fixed to the 1860 value. Simulations from 1861-2014 were done with varying annual CO_2 concentration values, and varying land use patterns according to the HYDE dataset, and with transient climate from 1901 until 2014.

2.6 LPX

Land-use change, including shifting cultivation and wood harvesting, is implemented as described in[15], using the full land-use transition and wood harvesting data provided [4]. Wood (heartwood and sapwood) removed by harvesting and land conversion is diverted to products pools with turnover rates of 2 years (37.5%) and 20 years (37.5%). The rest, including slash from roots and leaves is respired within the same year.

Simulation results shown here are based on employing the GCP 2015 protocol and input data[2]. LPX includes interactive C and N cycling with N deposition and N fertiliser inputs [16]. Simulations with shifting cultivation and wood harvesting were spun up to equilibrium under land-use transitions and wood harvesting of year 1500 [15]. Varying land-use transitions and wood harvesting was included from 1500 onwards, with CO_2 and N deposition of year 1860 and recycled climate from CRU TS 3.23, years 1901-1931. All simulations are done on a 1 x 1 degree spatial resolution and make use of monthly climate input. Original GCP standard input files were aggregated to 1 x 1 degrees conserving area-weighted means (climate input) or absolute area of cropland and pasture (land use input).

2.7 OCN

The OCN version used here is applied as in the framework of the annual carbon budget [2]. OCN includes interactive C and N cycling with N deposition and N fertiliser inputs [17]. Wood harvest was implemented by first satisfying the prescribed wood extraction rate from wood production due to land-use change, and then removing additional biomass proportionally from forested tiles. Wood (heartwood and sapwood) removed by harvesting and land conversion is diverted to products pools with turnover rates of 1 years (59.7%), 10 years (40.2% for tropical, and 29.9% for extratropical trees) and 100 years (10.4 % for extratropical trees)[18]. The remainder enters the litter pools. In case OCN's forest growth rate did not suffice to meet the prescribed wood extraction rate, harvesting was limited to 5% of the total stand biomass and assumed to stop if the stand biomass density fell below 1 kg C m^{-2}. These limits were set to account for offsets in annual wood production between OCN's predicted biomass growth and the assumptions in the Hurtt et al. database [4]. These limits may lead to lower than prescribed wood harvest rates in low productive areas. An additional run was performed with keeping wood harvest constant at 1860s level.

Simulations with wood harvesting were spun up to equilibrium using harvesting of the year 1860 [2]. Varying land-use transitions or wood harvesting was included from 1860 onwards, with CO_2 and N deposition of year 1860 and recycled climate from CRU-NCEP, years 1901-1931. All simulations are done on a 1 x 1 degree spatial resolution and make use of daily climate input, which is disaggregated to half-hourly values by means of a weather generator [19]. Original GCP standard input files were aggregated to 1 x 1 degrees conserving area-weighted means (climate input) or absolute area of cropland and pasture (land use input).

2.8 ORCHIDEE

WH: Developments to the version included in [2] include annual wood harvest, the total wood harvested of a grid cell is removed from above-ground biomass of the different forest PFTs proportional (i) to its fraction in the gridcell and (ii) also to its relative biomass among forest PFTs. This results in harvesting more wood in biomass-rich forests. In cases of inconsistencies between the Orchidee and Hurtt forest fraction, and to avoid forest being degraded from excessive harvest we assume that no more than 20% of the total forest biomass of a gridcell can be harvested in one year. Hence the biomass actually harvested each year can be slightly lower than prescribed [4]. The harvested biomass enters 3 pools of 1, 10 and 100 residence years respectively (and is part of F_{LULCC}). Model runs were done at 0.5°x0.5° resolution. Spin-up used recycled climate of 1901-1910. CO_2 concentration, land-cover and wood-harvest we those of the year 1860. The model was run until the change in mean total carbon of 98% of grid-points over a ten-year spin-up period was < 0.05%.

SC: Land cover transition matrices are upscaled from 0.5° LUH1 data [4] so no transition information is lost in the low-resolution run. The minimum bi-directional fluxes between two land cover types in LUH1 were treated as shifting cultivation. The model was forced with CRU-NCEP forcing (v5.3.2), re-gridded to 5° resolution from the original 0.5° resolution. Spin-up simulation used recycled climate data for 1901-1910 with atmospheric CO_2 held at 1750 level, and land cover fixed at 1500. Transient runs started from 1501 until 2014, with CO_2 varying from 1750 and climate varying from 1901. In the transient run for the control simulation, land cover is held constant at 1500; for the *SC* run, land cover varies by applying annual land use transition matrices of shifting cultivation. All runs have been performed with outputs on annual temporal resolution but forcing data is with 6-hourly.

2.9 OSCAR

A complete description of OSCAR v2.2 is provided by [20]. OSCAR is not a DGVM, but a compact Earth system model calibrated on complex models. Here, it is used in an offline setup in which the terrestrial carbon-cycle module is driven by exogenous changes in atmospheric CO_2 (IPCC AR5 WG1 Annex 2), climate (CRU TS v. 3.23), and land-use and land cover (HYDE 3.2).

The global terrestrial biosphere is disaggregated into 9 regions (detailed by [21]) and subdivided into 5 biomes (bare soil, forest, shrubland+grassland, cropland, pasture). The carbon-cycle in each of these 45 subparts is represented by a three-box model whose parameters are calibrated on DGVMs. The preindustrial equilibrium (carbon densities and fluxes) is calibrated on TRENDY v2 models [1]. The transient response of NPP, heterotrophic respiration and wildfires to CO_2 and/or climate is calibrated on CMIP5 models [22]. The impact of land-use and land-cover change on the terrestrial carbon-cycle is modelled using a book-keeping approach. Coefficients used to allocate biomass after land-use or land-cover change are based on [23].

Since OSCAR v2.2 is meant to be used in a probabilistic setup we made an ensemble of 2400 simulations in which the parameters (e.g. preindustrial equilibrium, transient responses, allocation coefficients) are drawn randomly from the pool of available parameterizations. See [20] for more details. The resulting "OSCAR" values discussed and shown in the main text are the median of this ensemble.

2.10 VISIT

Implementation of climate, land-use change (gross transitions, *SC*) and wood harvest (*WH*) has not changed from [2]. Land-use, land-use change, and wood harvest data for 1860-2014 were from LUH1 [4]. For *WH*, the amount of harvested biomass prescribed in [4] were transferred from simulated stem biomass to 1-year product pool (emitted in entirety in same year of wood harvest), 10-year product pool, and 100-year product pool in a same manner as in the cleared biomass with land-use change described in [24]. Non-harvested part of biomass were remain in the ecosystem. The fluxes from wood harvest pools are included in the NBP calculations.

Climate data was 1901-2014 monthly CRU TS v. 3.23 and all simulations were conducted with 0.5° spatial resolution. The model spin-up was performed recycling climate data from 1901-1920, and with land use patterns and CO_2 concentrations fixed to the 1860 value. Simulations from 1860-2014 were done with varying annual CO_2 concentration values, varying land use patterns according to LUH1, recycling the climate from 1901-1920 in the period 1860-1900, and with transient climate from 1901 until 2014.

3) Data in Figure 3

Data for net forest change from FAO [25] is calculated as the difference of forest area between 2000 and 2010 in each region. The same data were also used in the Houghton et al. bookkeeping model [26]. The net forest change from Hansen et al. [27] is based on satellite observations, and is their difference between gross forest gain and gross forest loss during 2000-2012. Because the LUH1 data set [4] only has one type of natural vegetation, and does not separate natural forest from natural grassland, the change in Figure 3 represents the total change of natural land. In Figure 3b, for LUH1 the gross loss includes transitions from primary/secondary vegetation to cropland / pasture, while the gross gain is the sum of transitions from cropland and pasture to secondary land. With grasslands and forests treated as separate land-cover types in LUH2 (http://luh.umd.edu/), the change includes transitions from primary / secondary forest to cropland / pasture (gross loss) and transitions from cropland / pasture to secondary forest (gross gain). The net change for LUH1 or LUH2 is the difference between gross loss and gross gain. To be consistent with [27], the period calculated for LUH1 and LUH2 is also from 2000 to 2012.

References

1 Sitch, S. *et al.* Recent trends and drivers of regional sources and sinks of carbon dioxide. *Biogeosciences* **12**, 653-679 (2015).

2 Le Quere, C. *et al.* Global Carbon Budget 2015. *Earth System Science Data* **7**, 349-396 (2015).

3 Klein Goldewijk, L., Beusen, A., van Drecht, G. & de Vos, M. The HYDE 3.1 spatially explicit database of human-induced global land use change over the past 12,000 years. *Globl Ecol. Biogeogr.* **20**, 73–86 (2011).

4 Hurtt, G. C. *et al.* Harmonization of land-use scenarios for the period 1500-2100: 600 years of global gridded annual land-use transitions, wood harvest, and resulting secondary lands. *Clim. Change* **109**, 117-161 (2011).

5 Clark, D. B. *et al.* The Joint UK Land Environment Simulator (JULES), model description – Part 2: Carbon fluxes and vegetation dynamics. *Geosci. Model Dev.* **4**, 701-722 (2011).

6 Wilkenskjeld, S., Kloster, S., Pongratz, J., Raddatz, T. & Reick, C. H. Comparing the influence of net and gross anthropogenic land-use and land-cover changes on the carbon cycle in the MPI-ESM. *Biogeosciences* **11**, 4817-4828 (2014).

7 Smith, B. *et al.* Implications of incorporating N cycling and N limitations on primary production in an individual-based dynamic vegetation model. *Biogeosciences* **11**, 2027-2054 (2014).

8 Pugh, T. A. M. *et al.* Carbon emission from land-use change is substantially enhanced by agricultural management. *Environmental Research Letters*, 124008 (2015).

9 Bayer, A. D., Lindeskog, M., Pugh, T. A. M., Fuchs, R. & Arneth, A. Uncertainties in the land use flux resulting from land use change reconstructions and gross land transitions. *Earth Syst. Dyn. Disc.* (2016).

10 Jones, P. & Harris, I. University of East Anglia Climatic Research Unit, CRU TS3. 21: Climatic Research Unit (CRU) Time-Series (TS) Version 3.21 of High Resolution Gridded Data of Month-by-month Variation in Climate (Jan. 1901—Dec. 2012). *NCAS British Atmospheric Data Centre* (2013).

11 Cosby, B. J., Hornberger, G. M., Clapp, R. B. & Ginn, T. R. A STATISTICAL EXPLORATION OF THE RELATIONSHIPS OF SOIL-MOISTURE CHARACTERISTICS TO THE PHYSICAL-PROPERTIES OF SOILS. *Water Resources Res.* **20**, 682-690 (1984).

12 Bondeau, A. *et al.* Modelling the role of agriculture for the 20th century global terrestrial carbon balance. *Glob. Change Biol.* **13**, 679-706 (2007).

13 Fader, M., von Bloh, W., Shi, S., Bondeau, A. & Cramer, W. Modelling Mediterranean agro-ecosystems by including agricultural trees in the LPJmL model. *Geosc. Model Dev.* **8**, 3545-3561 (2015).

14 Waha, K., van Bussel, L. G. J., Müller, C. & Bondeau, A. Climate-driven simulation of global crop sowing dates. *Glob. Ecol. Biogeogr.* **12**, 247–259 (2012).

15 Stocker, B. D., Feissli, F., Strassmann, K. M., Spahni, R. & Joos, F. Past and future carbon fluxes from land use change, shifting cultivation and wood harvest. *Tellus B,* **66**, 23188 (2014).

16 Stocker, B. D. *et al.* Multiple greenhouse-gas feedbacks from the land biosphere under future climate change scenarios. *Nat. Clim. Change* **3**, 666-672 (2013).

17 Zaehle, S., Ciais, P., Friend, A. D. & Prieur, V. Carbon benefits of anthropogenic reactive nitrogen offset by nitrous oxide emissions. *Nat. Geosc.* **4**, 601-605 (2011).

18 McGuire, A. D. *et al.* Carbon balance of the terrestrial biosphere in the twentieth century: Analysis of CO_2, climate and land use effects with four process-based ecosystem models. *Glob. Biogeochem. Cycles* **15**, 183-206 (2001).

19 Krinner, G., Ciais, P., Viovy, N. & Friedlingstein, P. A simple parameterization of nitrogen limitation on primary productivity for global vegetation models. *Biogeosciences Discussions* **2**, 1243-1282 (2005).

20 Gasser, T. *et al.* The compact Earth system model OSCAR v2.2: description and first results. *Geosc. Model Dev.* **submitted** (2016).

21 Houghton, R. A. & Hackler, J. L. Carbon flux to the atmosphere from land-use changes: 1850 to 1990. (Carbon Dioxide Information Analysis Center, Oak Ridge, Tennessee, 2001).

22 Arora, V. K. *et al.* Carbon-Concentration and Carbon-Climate Feedbacks in CMIP5 Earth System Models. *J. Clim.* **26**, 5289-5314 (2013).

23 Mason, E. J., Yeh, S. & Skog, K. E. Timing of carbon emissions from global forest clearance. *Nature Clim. Change* **2**, 682-685 (2012).

24 Kato, E., Kinoshita, T., Ito, A., Kawamiya, M. & Yamagata, Y. Evaluation of spatially explicit emission scenario of land-use change and biomass burning using a process-based biogeochemical model. *J. Land Use Sc.* **8**, 104-122 (2013).

25 FAO. Global Forest Resources Assessment 2010. (2010).

26 Houghton, R. A. *et al.* Carbon emissions from land use and land-cover change. *Biogeosciences* **9**, 5125-5142 (2012).

27 Hansen, M. C. *et al.* High-Resolution Global Maps of 21st-Century Forest Cover Change. *Science* **342**, 850-853 (2013).

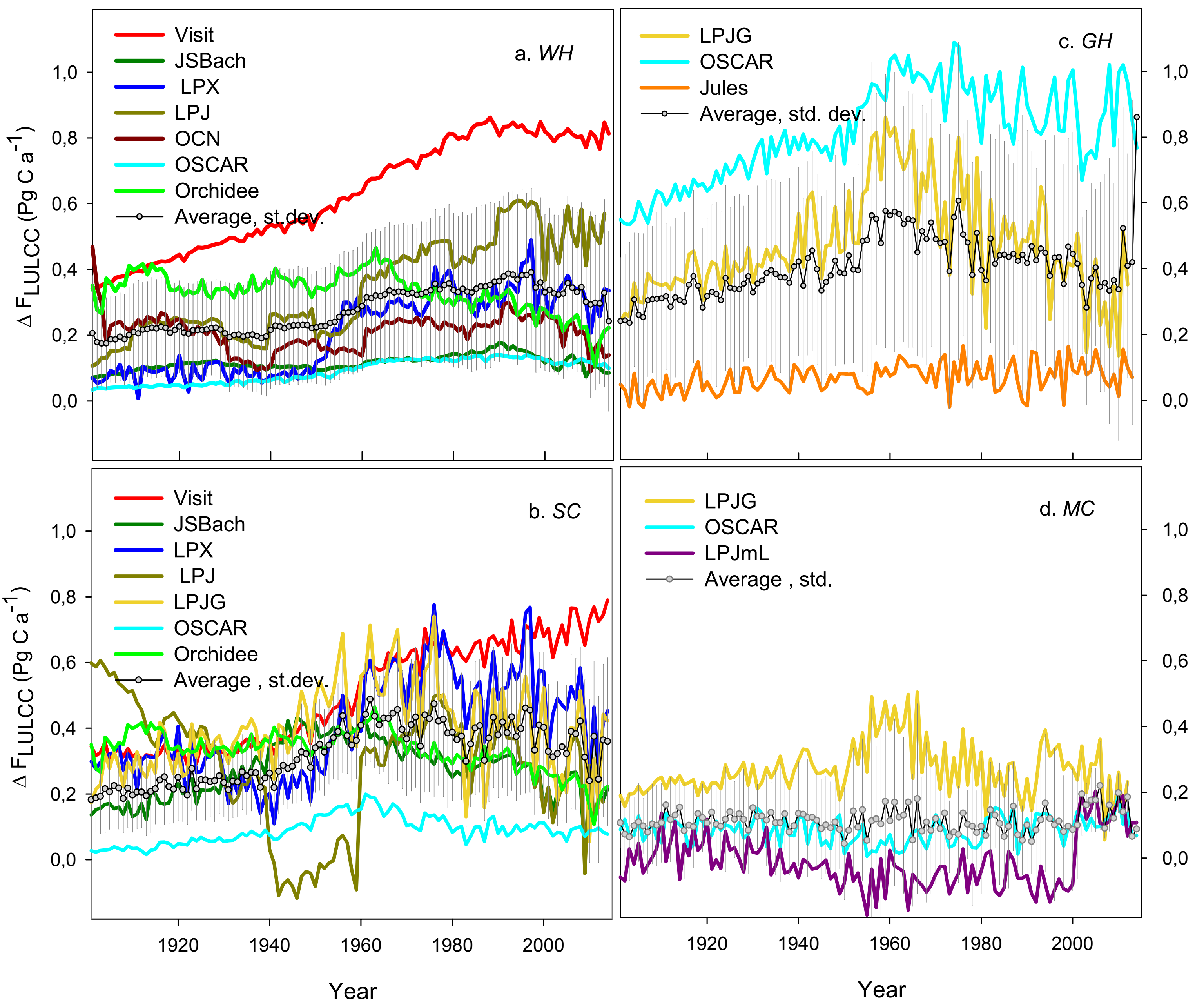
Visit
JSBach
LPX
LPJ
OCN
OSCAR
Orchidee
Average, st.dev.
a. *WH*
LPJG
OSCAR
Jules
Average, std. dev.
c. *GH*
Visit
JSBach
LPX
LPJ
LPJG
OSCAR
Orchidee
Average , st.dev.
b. *SC*
LPJG
OSCAR
LPJmL
Average , std.
d. *MC*
ΔF_{LULCC} (Pg C a^{-1})
0,0
0,2
0,4
0,6
0,8
1,0
1920
1940
1960
1980
2000
Year

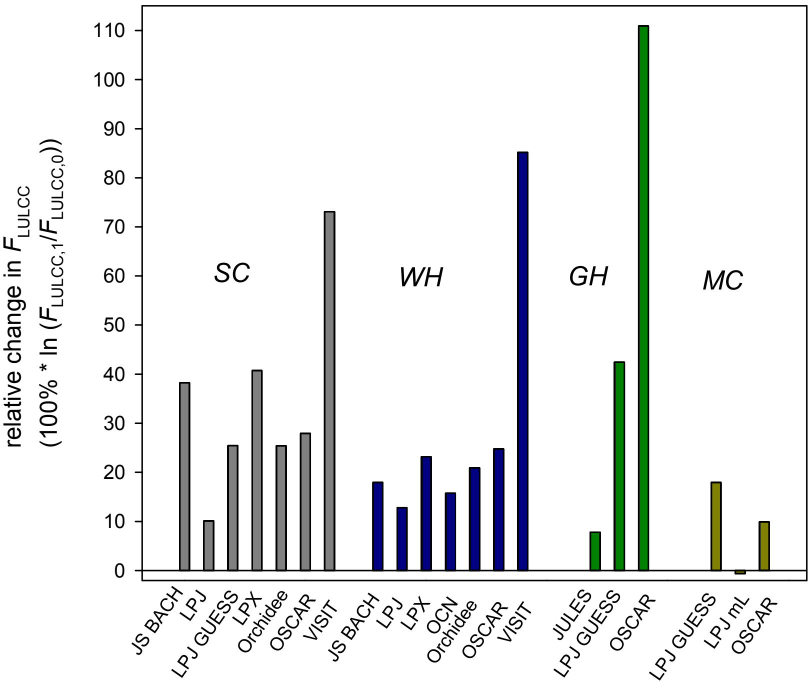
relative change in F_{LULCC}
(100% * ln ($F_{\mathrm{LULCC,1}}/F_{\mathrm{LULCC,0}}$))
0
10
20
30
40
50
60
70
80
90
100
110
SC
WH
GH
MC
JS BACH
LPJ
LPJ GUESS
LPX
Orchidee
OSCAR
VISIT
JS BACH
LPJ
LPX
OCN
Orchidee
OSCAR
VISIT
JULES
LPJ GUESS
OSCAR
LPJ GUESS
LPJ mL
OSCAR

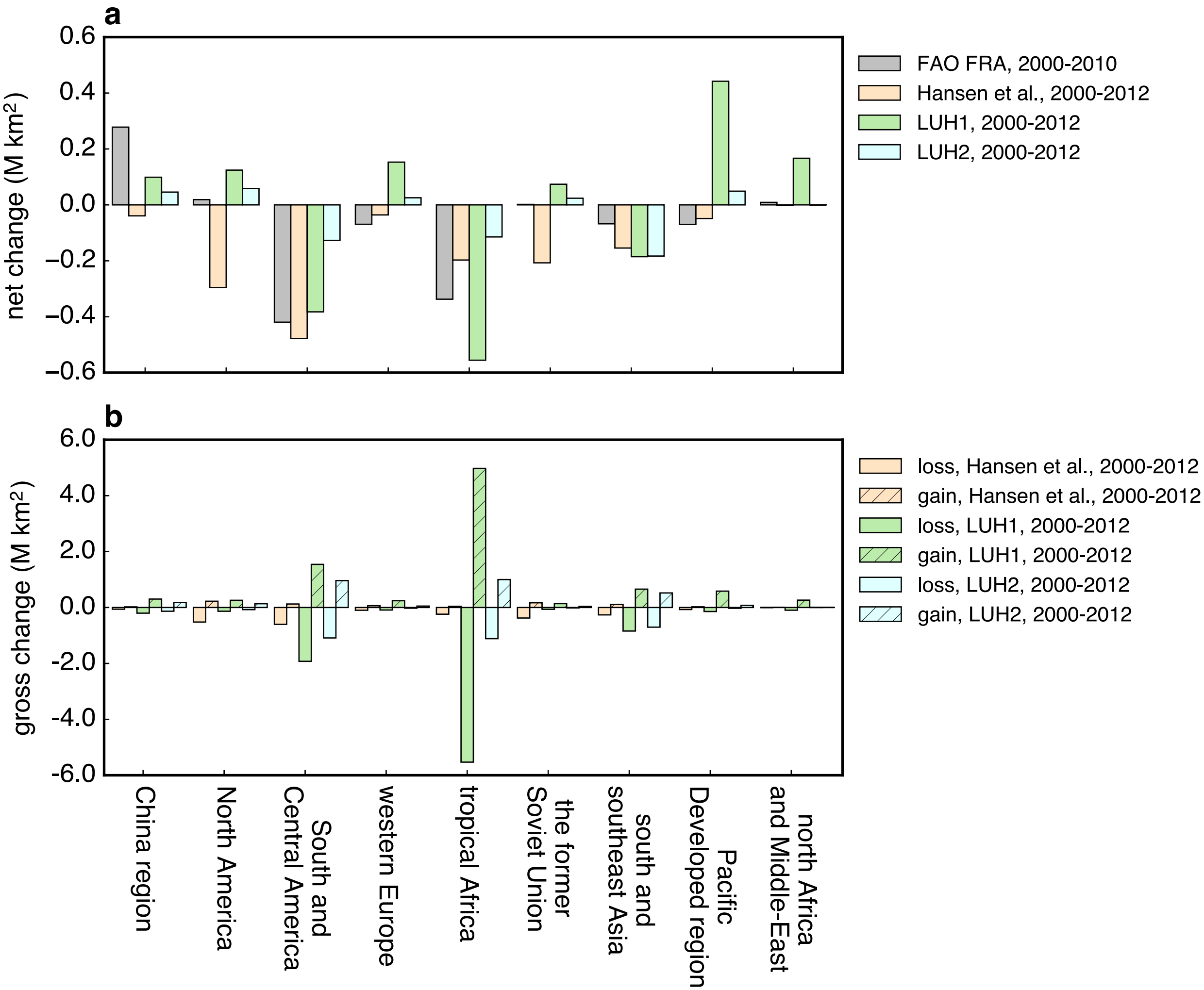
a
0.6
0.4
0.2
0.0
−0.2
−0.4
−0.6
net change (M km^2)
FAO FRA, 2000-2010
Hansen et al., 2000-2012
LUH1, 2000-2012
LUH2, 2000-2012
b
6.0
4.0
2.0
0.0
-2.0
-4.0
-6.0
gross change (M km^2)
loss, Hansen et al., 2000-2012
gain, Hansen et al., 2000-2012
loss, LUH1, 2000-2012
gain, LUH1, 2000-2012
loss, LUH2, 2000-2012
gain, LUH2, 2000-2012
China region
North America
South and Central America
western Europe
tropical Africa
the former Soviet Union
south and southeast Asia
Pacific Developed region
north Africa and Middle-East